Civil and Environmental Science Journal
Vol. 05, No. 02, pp. 118-128, 2022

Bearing capacity of large drilled shafts fully embeded in claystone and sandstone layers

Muhammad An Al Marwaji [1], **Yulian Firmana Arifin** [2,3*]

[1] Senior Geotechnical Engineer, Banjarmasin, Indonesia.
[2] Engineer Profesion Education, University of Lambung Mangkurat, Banjarbaru, 70714, Indonesia.
[3] Wetland Based Material Research Center, University of Lambung Mangkurat, Banjarmasin, 70123, Indonesia.

*y.arifin@ulm.ac.id

Received 20-04-2022; accepted 27-09-2022

Abstract. This paper analyzes the bearing capacity of large-diameter drilled shafts fully embedded in the claystone and sandstone layers. The foundations used are the drilled shafts for the Pulau Balang bridge pylons built across the Balikpapan bay. Three bored pile foundations with a planned diameter of 2 meters by 60 meters were used. The bearing capacity of the foundation in the field was carried out using the Osterberg cell test. The foundation's upper side's bearing capacity is 32.77, 27.26, and 114.46 MN, and the lower parts are 26.98, 27.16, and 50.25 MN, respectively. The results show that the method closest to the upper part of the OC test is the method suggested by Kulhawy and Phoon, with a value of C = 0.5. As for the lower part, the closest approach combines the Kulhawy and Phoon and the Rowe and Armitage methods. The Kulhawy and Phoon (1993) and Rowe and Armitage (1987) methods for the main claystone layer and the O'Neil and Reese (1993) and Rowe and Armitage (1987) methods for the main sandstone layer are the combinations of methods that come close to the total bearing capacity of the field.

Keywords: claystone, sandstone, drilled shaft, bearing capacity, Osterberg cell test.

1. Introduction

Analysis of the bearing capacity of the foundation of drilled shafts requires a very high cost for both the implementation and the instrumentation. Thus, many formulas are made based on data from field testing results in large construction projects. Researchers need to help publicize existing methods' use to get more information about how reliable and valid these methods are for a certain situation.

Numerous approaches have been presented for determining the bearing capacity of the shaft and foundation end. These methods consider many things, such as parameters of rock strength, rock mass stiffness, and interface roughness [1], the possibility of slip occurring at the pier–rock interface under load conditions [2], and the discontinuity effect [3]. Carrubba [4] says that the pile's response during axial load depends on the strength of the rock, the length of the socket in the rock layer, and the length of the shaft in the soil. Some of them suggested new methods, some made modifications, and some reported the suitability of using those methods. The most common formula for conducting analysis is to match the computation with the results of field tests such as the loading test [1]–[3] and the biaxial test

[5]. O'Neil [6] states that calculating the bearing capacity of piles requires sharp knowledge of the significant geotechnical effects and construction phenomena and the performance of foundations designed in related geological formations. Therefore, publishing a bearing capacity analysis is recommended, especially for massive constructions.

This study uses the results of testing the bored pile foundation on the construction of the Balang Island bridge, connecting Penajam Paser Utara Regency, which has been decided as the new capital of Indonesia, with Tempadung, Balikpapan Municipality in East Kalimantan. The Balang Island bridge superstructure is a two–to 402 m long stayed bridge with two pylons standing on four pile caps and 144 bored piles in total. Balang Island has two pile caps and two more on the Tempadung side. Steel pipe casings protect the top of the seabed, but the rest of the piles, all the way to the bottom, are unprotected. Bored piles are installed in the sandstone and claystone layers. There are 144 bored piles in total. Two pile caps are located on Balang Island, and two others are on the Tempadung side. Bored piles are designed using steel pipe casings for the top of the seabed, and the rest of the piles, up to the bottom, do not use protection. Some bored piles are installed in the sandstone and claystone layers.

The drill tools used were Zhongrui Airlift, Buma Airlift, and Zhongrui Suction, with a diameter of 1.8 m. There is no difference between the design and the actual diameter of the part mounted to the casing. However, there is an indication of a change in diameter at the bottom without the casing. The amount of concrete used in the construction process demonstrates this. Necking, which results in a smaller pile diameter, and bulging, which results in a larger pile diameter, are two examples of this change in diameter.

Although the pile's diameter increases due to bulging, this phenomenon is still considered damage to the foundation. Chan [7] reports that mixing soil material due to the collapse of the hole wall can result in a reduced pile bearing capacity. Wakil and Kassim [8] stated that bulging can increase the bearing capacity of the foundation even though it is still considered a defect in the pile. Therefore, changes in diameter are also considered in this analysis.

Pile integrity tests must be carried out to ensure that no other material is mixed with concrete due to the collapse of the hole wall [7]. Crosshole sonic logging (CSL) is one method for checking pile integrity. This method has proven accurate and reliable for finding pile defects [9]. In this project, the same process (i.e., CSL) was carried out, and no abnormalities were found in the boring pile shaft.

The method commonly used to obtain the field-bearing capacity of bored piles located above the sea is the Osterberg cell test (OC test), also known as the biaxial test method [10] [11]. In constructing the Suramadu bridge in Indonesia, this method determined how much load the large diameter borings could hold [5]. The purpose of this article is to analyze the bearing capacity of bored pile foundations using commonly used formulas. Three bored piles were used, each with biaxial test instruments. Changes in diameter as a result of the drilling process are also considered.

2. Material and Methods

2.1. Geomaterial Properties

Two deep borings with undisturbed sampling located close to the piles tested were performed, namely BH−1 and BH−2. The geotechnical rock properties obtained from BH−1 and BH−2, including unit weight, unconfined compression (q_u), rock quality designation (RQD), rock mass modulus of elasticity (E_{mass}), and the ratio between rock mass and intact rock secant modulus of rock, are presented in Figures 1(a), 1(b), 2(a), and 2(b), respectively. In addition, samples were taken to determine the RQD of the rock formations, which is one of the most important factors in determining the bearing capacity of the shaft.

The two test points exhibit significantly different data, with BH−1 demonstrating the dominant soil layer as claystone, while BH−2 demonstrates the dominant soil layer as sandstone. The qu in BH−1 is less than 4 MPa than the qu in BH−2, reaching a value of 10 MPa. RQD is also higher on the BH−2 than it is on the BH−1. E_{mass} attains a pressure of 1000 MPa in BH−2. The E_{mass} in BH2 is significantly larger than in BH1, reaching a peak of only 300 MPa.

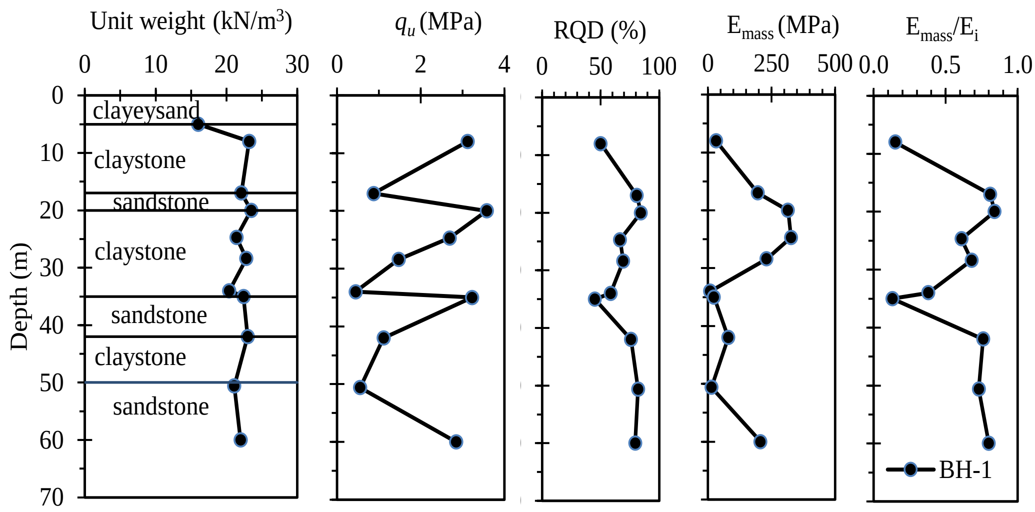

Figure 1. Geotechnical rock properties of BH–1

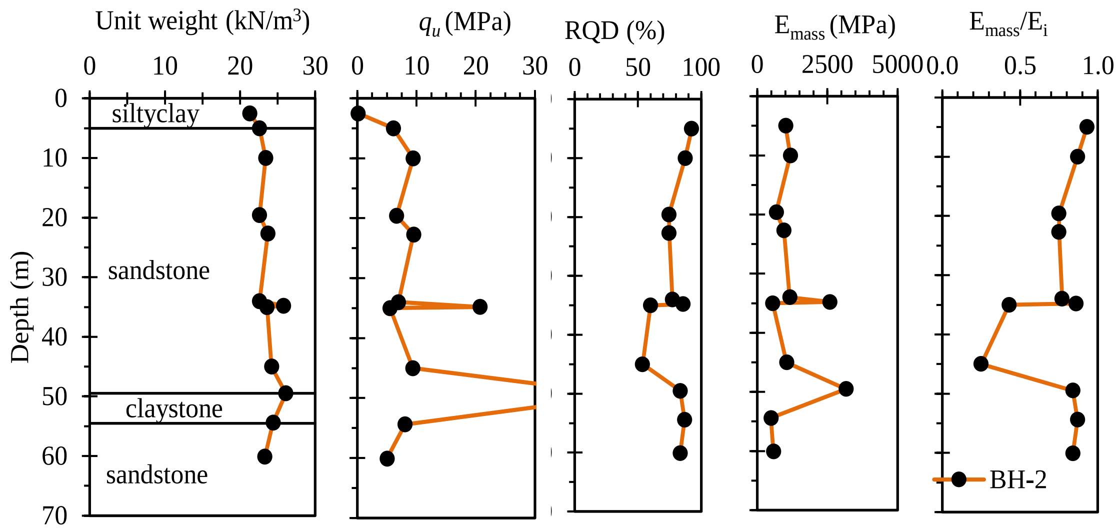

Figure 2. Geotechnical rock properties of BH–2

2.2. Osterberg Cell Test

Three OC tests were performed on three piles with a diameter of 2 m, named Pile–1, Pile–2, and Pile–3, with a total length of 68.68 m, 68.68 m, and 53.8 m, respectively. In the implementation of OC test work, the loadcell is placed at a relatively different level for each pile tested. For example, the load cell of Pile–1 is located at 57.68 m from the pile head. For Pile–2 and Pile–3, loadcells are placed at a depth of 57.7 m and 44.8 m, respectively.

Figures 3(a) and 3(b) show the sketches of loadcell locations in the foundations for Pile–1, Pile–2, and Pile–3, respectively. This resulted in each loadcell receiving a load due to the overlying concrete of 2627 kN, 2626 kN, and 2040 for Pile–1, Pile–2, and Pile–3, respectively. Loading and unloading were carried out according to ASTM D1143–81 [12] (i.e., a quick load test for individual piles) with a maximum load of 2×18,000 kN. The maximum load is determined based on the capacity that must be held by each 18000 kN pile.

Civil and Environmental Science Journal
Vol. 05, No. 02, pp. 118-128, 2022

3. Results and Discussions

Figure 4 shows the OC test results for the three foundations, which are indicated by the relationship between load and displacement. The maximum upward displacement of each pile at a load of 18000 kN is 1.7 mm, 5.67 mm, and 2.93 mm for Pile–1, Pile–2, and Pile–3. The maximum downward displacement for Pile–1, Pile–2, and Pile–3 is 3.75 mm, 6.92 mm, and 6.13 mm, respectively, at a maximum load of 18000 kN. However, the maximum load given is not the maximum load at collapse. Failure load was determined based on the criteria adopted by FHWA [13], which is located at a displacement of 5% of the foundation diameter (0.05D) if the shaft plunging cannot be achieved. This criterion looks at the statistical tests that are the easiest and most reliable compared to methods like Davisson, De Beer, and curve shape [14].

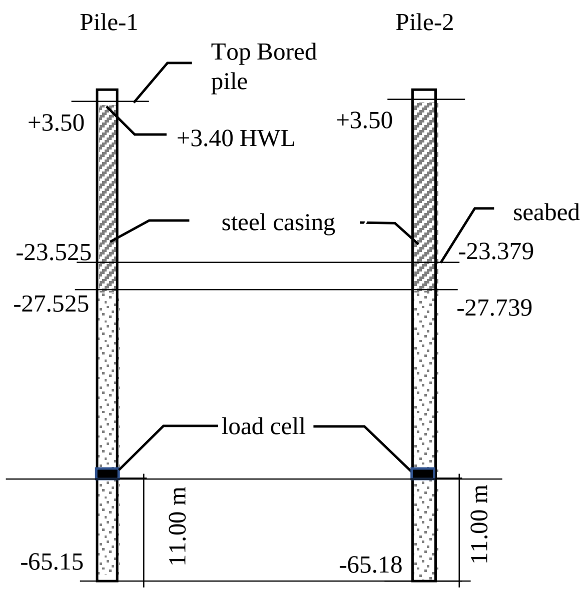

Figure 3. Sketchs of pile and load cell positions Pile–1, Pile–2, and Pile–3

The relationship curves between load and displacement in Figure 4 were fitted by the equation suggested by Carubba [4]. The model is based on a hyperbolic transfer function approach (Equation 1).

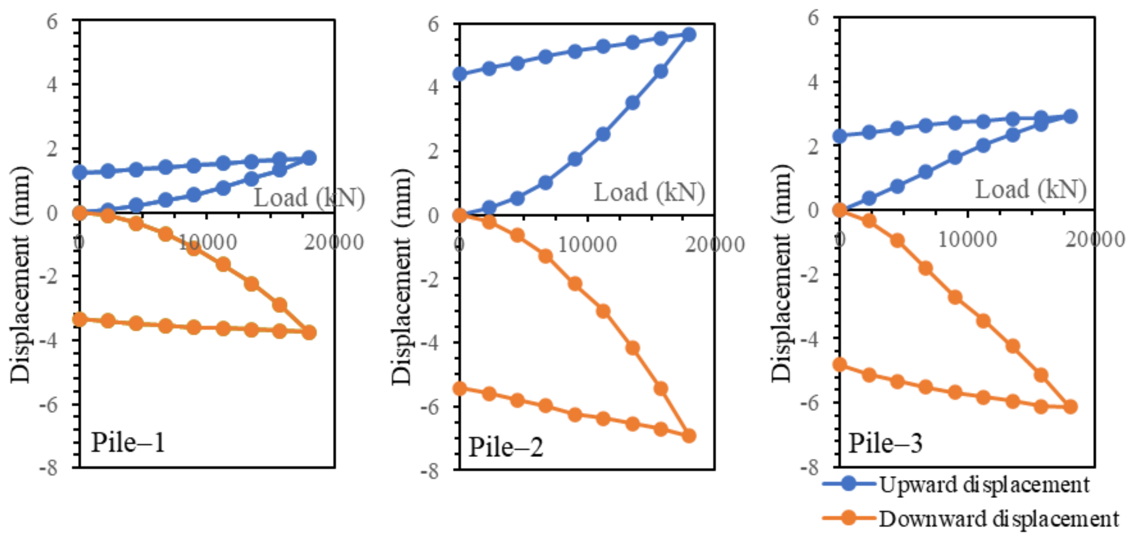

Figure 4. Upward and downward displacement obtained from OC tests

Civil and Environmental Science Journal
Vol. 05, No. 02, pp. 118-128, 2022

$$f(z) = \frac{w(z)}{a+bw(z)} \quad (1)$$

where: f(z) is the mobilized resistance along a shaft portion or at the shaft base, and w(z) is the corresponding displacement. The ɑ is the reciprocal of the initial slope parameter, and the b is the limit strength parameter. Using Equation 1 and the failure load at 0.05D, the OC test's bearing capacity can be found in Table 1.

Table 1. Bearing capacity of shafts predicted from OC tests data

Pile	Upward			Downward			Total	
	1/a	1/b	Q_s (MN)	1/a	1/b	Q_e *) (MN)	(MN)	(kN)
1	22.44	33.26	32.77	12.67	27.57	26.98	59.75	59,750
2	7.97	28.23	27.26	6.58	28.33	27.16	54.42	54,420
3	6.00	141.46	114.46	4.21	57.05	50.25	194.70	194,700

*) including side resistance of shaft under loadcell

3.1. Determination of Actual Diameter of Bored Pile

The actual diameter of the hole is not measured directly using a tool but is based on the volume of concrete embedded in the hole. The mean diameter is calculated using Equation 2.

$$D_{average} = \sqrt{\left(\left(\frac{\Delta V}{\Delta H}\right) * \frac{4}{\pi}\right)} \quad (2))$$

where ΔV is the volume of the concrete inserted into the borehole, and ΔH is the depth difference before and after the concrete is shed (after the tremie is spaced). Figure 5 is an example of the average diameter calculated using Equation 2. Pile Cap 1 and Pile Cap 2 (close to BH–1) are located on one pylon, while Pile Cab 3 is located on another (close to BH–2). In Figure 5, D1–34, D1–69, and D2–35 are Pile–1, Pile–2, and Pile–3, respectively. Generally, the shaft diameter is larger than the design diameter (i.e., 2.00 m). The biggest change occurred at the base of the pile bores, caused by water flushing. The diameter of the piles' tips in Pile Cab–1 and 2 is greater than those in Pile Cab–3. This is because the two pile groups are located in the claystone layer at a depth of 40–50 m with q_u < 2 MPa (considerably weak). The Pile–3 base is located on a relatively hard sandstone layer at a depth of 35–40 m with a q_u of 5–10 MPa.

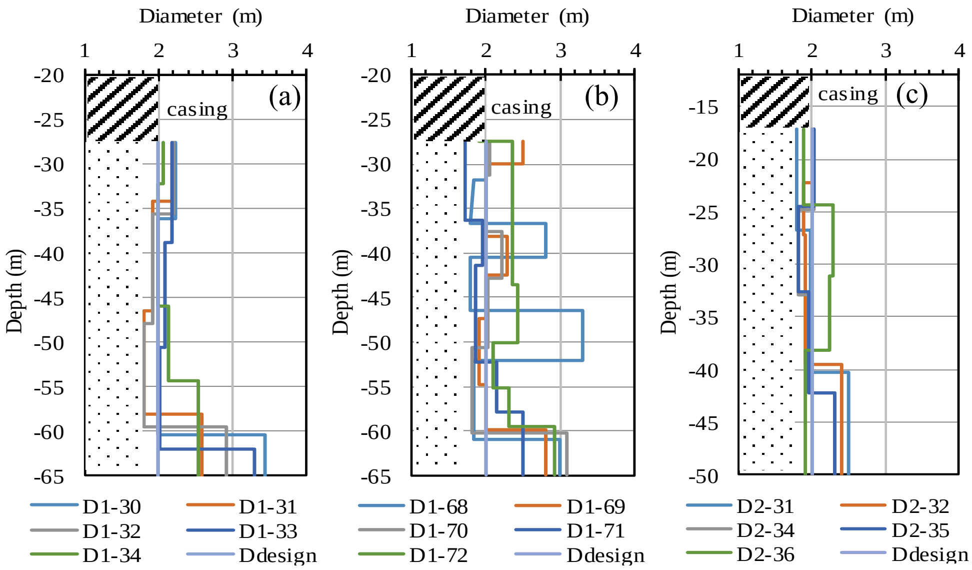

Figure 5. Calculated bore diameter (a) Pile Cab 1, (b) Pile Cab 2, and (c) Pile Cab 3.

3.2. Bored Pile Bearing Capacity

3.2.1. Bearing capacity of the upper side of the load cell

Several methods have been suggested for calculating bored pile bearing capacity. One formula often used is recommended by O'Neill and Reese [15] (Equation 3). This approach was applied by AASHTO and numerous other studies to determine the bearing capacity of drilled piles [10], [13], [16].

$$\frac{f_s}{p_a} = 0.65\ \alpha_R \sqrt{\frac{q_u}{p_a}} \tag{3}$$

where: f_s denotes friction resistance and p_a is the atmospheric pressure of 101.3 kPa. q_u is the mean value of uniaxial compressive strength for the rock layer, and α_E is an empirical reduction factor which is a function of the estimated ratio of rock mass modulus to the modulus of intact rock (E_M/E_R). The value depends on the RQD of the rock, as shown in Table 2, and the reduction factor is obtained from Table 3.

Table 2. Modulus Ratio (E_M/E_R) based on RQD (O'Neill et al.) [17]

RQD (%)	E_M/E_R Closed Joint	E_M/E_R Open Joints
100	1.00	0.60
70	0.70	0.10
50	0.15	0.10
20	0.05	0.05

Table 3. Reduction faktor (α_R) (O'Niell and Reese) [15]

E_M/E_R	α_R
1.0	1.0
0.5	0.8
0.3	0.7
0.10	0.55
0.05	0.45

Tables 4 and 5 illustrate the calculation process for the upper side bearing capacity component of Piles−1 and 2, respectively, using Equation 3. The total Q_s obtained are 50.795 kN and 48.328 kN. Using the same procedures as for Pile−3, the total Q_s acquired is 94.725 kN. As can be seen, the total Q_s obtained for Piles−1 and 2 are remarkably similar, owing to the use of the same drill data and nearly identical foundation diameters. However, the total Q_s of Pile 3 are nearly double that of the others because it was constructed on sandstone−dominated soil with higher q_u and RQD data.

Table 4. Bearing capacity calculation of Pile−1 using O'Neil et al. [17] method

L (m)	D (m)	q_u (MPa)	RQD (%)	E_M/E_R	α_R	f_s (kPa)	Q_s (kN)
5.0						Neglected	
7.1	2.26	3.50	65	0.67	0.87	335	16,791
4.9	2.26	3.50	65	0.67	0.87	335	11,745
1.1	2.17	3.58	84	0.84	0.93	366	2,653
1.9	2.17	3.58	84	0.84	0.93	366	4,839
4.7	2.17	2.69	68	0.75	0.89	304	9,632
1.4	2.2	1.47	68	0.75	0.89	224	2,233
3.9	2.20	0.44	59	0.48	0.78	108	2,902
						Total	50,795

Table 5. Bearing capacity calculation of Pile−2 using O'Neil et al. [17] method

L (m)	D (m)	q_u (MPa)	RQD (%)	E_M/E_R	α_R	f_s (kPa)	Q_s (kN)
5.0	2.07					Neglected	
5.0	2.07	3.50	65	0.66	0.86	333	10,916
7.0	2.00	3.50	65	0.66	0.86	333	14,554
3.0	2.00	3.58	84	1.19	1.08	423	7,978
3.6	2.00	2.69	68	0.75	0.89	304	6,952
2.4	2.13	1.47	68	0.75	0.89	224	3,541
6.0	2.13	0.44	59	0.50	0.79	108	4,387
						Total	48,328

Williams and Pells [1] suggested using the line of best fit of the α and q_u data for mudstone, shale, and sandstone (Equation 4). Several studies have used this equation to assess the bearing capacity of bored piles [18]–[21]. A graph digitizer and a statistical analyzer were used to fit the data that can be approximated by Equation 5. Moreover, the β is determined using a best−fit equation, as shown in Equation 6. The effect of β is negligible when the mass modulus is close to the intact modulus. Williams and Pells [1] proposed a safety factor of 2.5 to reduce the effect of scattering data to obtain α. A is a reduction factor for rock socket skin friction, and β is a reduction factor for discontinuity.

$$f_s = \alpha\, \beta\, q_u \tag{4}$$

$$\alpha = 0.107 + \frac{0.351}{q_u} \tag{5}$$

$$\beta = 0.043 + 0.96\left({E_m}/{E_i}\right)^{0.328} \tag{6}$$

However, Alshenawy et al. [22], Stark et al. [16], and Rezazadeh and Eslami [23] used an equation that Kulhawy and Phoon [22] came up with to get the shaft side shear that is written in Equation 7.

$$\frac{fs}{pa} = C\sqrt{\frac{qu}{2pa}} \tag{7}$$

where q_u is the uniaxial compressive strength, p_a is atmospheric pressure equal to 101.3 kPa, and C is a dimensionless factor reflecting variations in the intact strength and roughness of the rock. Sockets that are artificially roughened have a lower limit of C = 0.5, a reasonable lower limit of 1, a mean of 2, and an upper limit of 3. Tables 6 and 7 summarize the example results of the two methods for calculating the friction bearing capacity of the bored pile. The results obtained are much different from the two approaches. The results are almost four times as different as the two approaches. It can be seen that Kulhawy and Phoon's method [22] is highly dependent on the α. If the average value is used (i.e., 2), the f_s obtained is 126.133 kN, which is close to that analyzed using Williams and Pell's approach [1].

Table 6. Bearing capacity calculation of Pile−1 using Williams and Pells [1]

L (m)	D (m)	q_u (MPa)	E_m/E_i	α_R	β	f_s (kPa)	Q_s (kN)
5.0						Neglected	
7.1	2.26	3.50	0.48	0.27	0.80	755	37,842
4.9	2.26	3.50	0.80	0.27	0.94	885	31,038
1.1	2.17	3.58	0.84	0.27	0.95	911	6,606
1.9	2.17	3.58	0.84	0.27	0.95	911	12,051
4.7	2.17	2.69	0.61	0.30	0.86	695	22,037
1.4	2.2	1.47	0.68	0.41	0.89	534	5,315
3.9	2.20	0.44	0.38	0.97	0.74	316	8,519
						Total	123,408

Table 7. Bearing capacity calculation of Pile−1 using Kulhawy and Phoon [22]

L (m)	D (m)	q_u (MPa)	RQD (%)	C	f_s (kPa)	Q_s (kN)
5.0					Neglected	
7.1	2.26	3.50	65	0.50	211	10,558
4.9	2.26	3.50	65	0.50	211	7,385
1.1	2.17	3.58	84	0.50	213	1,544
1.9	2.17	3.58	84	0.50	213	2,816
4.7	2.17	2.69	68	0.50	185	5,855
1.4	2.2	1.47	68	0.50	136	1,357
3.9	2.20	0.44	59	0.50	75	2,013
					Total	31,528

3.2.2. Bearing capacity of the lower side of the load cell

Two components must be analyzed at the bottom side of this load cell, i.e., side friction and end-bearing capacities. Shaft friction is calculated by using the three methods above, i.e., O'Neil et al. [17], Williams and Pells [1], and Kulhawy and Phoon [22] methods (Equations 3–7). Table 8 summarizes all the calculation results, including upper and lower part calculations. This result is consistent with the results of the previous calculation, where the bearing capacity calculated by the William method yields the highest value, followed by O'Neil, and the smallest, which is analyzed by the Kulhawi method. Despite having the same pile lengths and calculations using the same soil data (i.e., BH1), Piles−1 and 2 have different bearing capacity values due to the difference in the installed diameter, as shown in Figure 5. Table 8 also shows that Pile−3 has the highest bearing capacity due to the dominant sandstone soil layer with shear strength parameters that exceed the data in Piles−1 and 2.

3.2.3. End bearing capacity

End bearings are calculated using the Rowe and Armitage [2], AASHTO [13], and Zhang and Einstien [3] formulas. Additionally, Rowe and Armitage [2][16] proposed an equation for determining the base shaft's maximum bearing capacity (Equation 8).

$$q_e = 2.5\ q_u \tag{8}$$

where q_e denotes the drilled shaft's end bearing.

Table 8. Summary of calculation results of skin friction bored piles

Methods	Upper side (kN)			Lower side (kN)		
	Pile–1	Pile–2	Pile–3	Pile–1	Pile–2	Pile–3
O'Neill and Reese [15]	50,795	48,328	94,725	17,014	21,424	29,456
Williams and Pells [1]	123,408	100,645	278,814	32,875	38,404	79,013
Kulhawy and Phoon [22] (C=0.5)	31,528	25,594	55,580	14,329	14,329	18,417

AASHTO [13] recommends calculating the end-bearing capacity using Equation 9.

$$q_e = N_{ms}\ q_u \tag{9}$$

where N_{ms} is a parameter related to the quality and type of rock mass. AASHTO [13] and Zhang [24] [25] provide detailed N_{ms} values.

Zhang and Einstien [3] [20] recommend equations to predict the end bearing capacity of drilled shafts socketed into rock based on the analytical relationship and field data tests. Equations 10–13 should be used to create a foundation with a minimum embedment ratio of 3.0 [3].

$$\text{Lower bound: } q_e = 3.0\ \sqrt{q_u} \tag{10}$$

$$\text{Upper bound: } q_e = 6.6\ \sqrt{q_u} \tag{11}$$

$$\text{Mean: } q_e = 4.8\ \sqrt{q_u} \tag{12}$$

Table 9 summarizes the results of the end-bearing capacity analysis using Equations 8–12. As can be seen from the table, the end bearing capacity calculated using the Rowe and Armitage [2] method yields the highest value. The remaining two, on the other hand, produce smaller values. The AASHTO method considers the rock RQD at the pile's tip, specified by the N_{ms} parameter. Piles– 1 and 2 have a combined RQD of 76%, with a good quality rock mass with an N_{ms} of 0.32. Meanwhile, at the end of Pile–3, the RQD is 53%, including the appropriate rock category with an N_{ms} of 0.075. This parameter significantly reduces the bearing capacity of the pile tip.

The third method recommended by Zhang and Einstien [3][20] is based on the rock's undrained compressive strength. So, even though the coefficient number used by Zhang and Einstein [3] is higher than in the other two methods, the result is the smallest bearing capacity.

Tabel 9. End bearing capacities using Zhang and Einstien [3]

Pile	Rowe and Armitage [2] (kN)	AASHTO [13] (kN)	Zhang and Einstien [3] (kN)
Pile–1	13,999.09	1,659.15	787.00
Pile–2	10,258.38	1,215.81	576.71
Pile–3	61,550.28	1,709.73	1,412.64

Based on the Osterberg cell test result, comparisons were made with calculations using the methods of O'Neill and Reese [15], Williams and Pells [1], and Kulhawy and Phoon [22]. For the upper side of the loadcell, the friction bearing capacity of Pile–1 and Pile–2 implanted in claystone dominant soil (q_u < 5 MPa) is very close to the results calculated by the Kulhawy and Phoon [22] method with C = 0.5. Likewise, pile–3 with a q_u > 5 MPa is very close to the value of C = 1.

For the upper side of the loadcell, the bearing capacity of friction Pile–1 and Pile–2 embedded in soil with claystone dominant (i.e., q_u < 5 MPa) is 32.77 MPa and 27.26 MPa, respectively. These are very close to the results of calculations by the Kulhawy and Phoon [22] method with C = 0.5 (i.e., 31.528 MPa and 25.594 MPa, respectively for Pile–1 and Pile–2). For Pile–3 with a q_u > 5 MPa, the OC test results (i.e., 114.46 MPa) are very close to the analytical results for the value of C = 1 (i.e., 111.16 MPa).

The shaft bearing capacity of a pile with a q_u < 5 MPa calculated by the method of O'Neill and Reese [15] produces 1.5–1.8 times greater than the results of the OC test. This method's calculations are closer to the bearing capacity of Pile–3 implanted in the dominant sandstone layer with a q_u > 5 MPa. This is in line with the value suggested by O'Neil [6], where the value is divided between soil and other materials at s_u/p_a = 2.5, or about 5.06 MPa.

By dividing the calculation results by a safety factor of 2.5 as Williams and Pells [1] suggested to reduce the scatter in the determination, the bearing capacities are 41.936 kN, 40.258 kN, and 111.526 kN for Pile–1, Pile–2, and Pile–3, respectively. Pile–3. The results of this calculation are close to the results of the OC test, but the condition of the OC test is the ultimate bearing capacity. Therefore, there must be a higher safety factor (e.g., five) for both conditions when William and Pells' method [1] is used.

The best way to figure out how the methods work together is to add up the frictional and pile-end bearing capacities, as shown in Table 10. Bold values indicate those that are closest to the total field bearing capacity. The closest combination of methods for piles constructed on a claystone dominant layer is a combination of methods by Kulhawy and Phoon [22] and Rowe and Armitage [2]. This combination makes a difference of 0.18 and 7.79 percent for Piles−1 and 2, respectively. In the Kulhawy and Phoon [22] method, the coefficient C significantly affects the side friction piles. In this analysis, the coefficient of C used is the lower limit of 0.5. While the end bearing is the Rowe and Armitage [2] method, which multiplies the undrained compressive strength of rock with an empirical coefficient of 2.5. For Pile-3, primarily installed on sandstone, the results of O'Neill et al. [17] and Rowe and Armitage [2] are the closest to the field.

Although the bearing capacity calculated from the data and field test results is generally divided by different safety factors, the factor for the field test results (i.e., 2) is generally smaller than the analysis result (at least 2.5) based on SNI 8460 [26]. Therefore, these findings are still appropriate for use.

Table 10. The combination of methods used in this study

	Pile−1a	Pile−2a	Pile−3a	Pile−1b	Pile−2b	Pile−3b	Pile−1c	Pile−2c	Pile−3c
Pile−1d	81,808			170,282			**59,856**		
Pile−2d		80,010			149,307			**50,181**	
Pile−3d			**185,731**			419,377			135,547
Pile−1e	69,468			157,942			47,516		
Pile−2e		70,968			140,265			41,139	
Pile−3e			125,891			359,537			75,707
Pile−1f	68,596			157,070			46,644		
Pile−2f		70,329			139,626			40,500	
Pile−3f			125,594			359,240			75,410

Note: a (O'Neill et al) [17], b (Williams and Pells) [1], c (Kulhawy and Phoon) [22], d (Rowe and Armitage) [2], e (AASHTO) [13], f (Zhang and Einstien) [3].

4. Conclusions

An analysis of the bearing capacity of large–diameter bored piles in claystone and sandstone layers has been presented. The following are some of the points that can be concluded:

1. In the analysis, the actual diameter of the bored pile in the field must be considered, particularly the diameter at the foundation's base.

2. For drilled shafts installed in claystone layers with a qu < 5 MPa, the bearing capacity of Pile–1 and Pile–2 upper sides is 32.770 kN and 27.260 kN, respectively. The method closest to this calculation is the method suggested by Kulhawy and Phoon (1993), with a value of C = 0.5.
3. The results of the upperside foundation in the sandstone layer with a qu > 5 MPa are most closely matched by the method of O'Neil and Reese (1993).
4. The bearing capacity of the bored pile analyzed by the Kulhawy and Phoon (1993) and Rowe and Armitage (1987) methods, namely for the frictional and tip resistances in the claystone dominant layer, is close to that obtained from field tests. In the sandstone layer, the best ways to figure out the shaft and end bearing capacity are those suggested by O'Neil and Reese (1993) and Rowe and Armitage (1987).

Acknowledgements
The authors would like to thank the Ministry of Public Works and Housing, especially CMO of the Pulau Balang Bridge Mr. Asyfak Bismoseno, for giving them information about the project.

References

[1] A. F. Williams and P. J. N. Pells, "Side Resistance Rock Sockets in Sandstone, Mudstone, and Shale.," *Can. Geotech. J.*, vol. 18, no. 4, pp. 502–513, 1981, doi: 10.1139/t81-061.
[2] R. K. Rowe and H. H. Armitage, "Design Method for Drilled Piers in Soft Rock.," *Can. Geotech. J.*, vol. 24, no. 1, pp. 126–142, 1987, doi: 10.1139/t87-011.
[3] L. Zhang and H. H. Einstein, "End bearing capacity of drilled shafts in rock," *J. Geotech. Geoenvironmental Eng.*, vol. 124, no. 7, pp. 574–584, 1998, doi: 10.1061/(ASCE)1090-0241(1998)124:7(574).
[4] P. Carrubba, "Skin friction on large-diameter piles socketed into rock," *Can. Geotech. J.*, vol. 34, no. 2, pp. 230–240, 1997, doi: 10.1139/cgj-34-2-230.
[5] M. Irsyam, A. Sahadewa, A. Boesono, and Soebagyo, "Pengaruh Strength Reduction Tanah Clay-Shale akibat Pelaksanaan Pemboran terhadap Nilai Daya Dukung Pondasi Tiang di Jembatan Suramadu Berdasarkan Analisis Hasil Tes OC," *J. Tek. Sipil*, vol. 14, no. 2, pp. 69–82, 2007.
[6] M. W. O'Neill, "Side Resistance in Piles and Drilled Shafts," *J. Geotech. Geoenvironmental Eng.*, vol. 127, pp. 3–16, 2001.
[7] H. C. Chan, "Non-Destructive Testing of Concrete Piles using the Sonic Echo and Transient Shock Methods," University of Edinburgh, 1987.
[8] A. Z. El Wakil and M. Kassim, "Bulging as a pile imperfection," *Alexandria Eng. J.*, vol. 49, no. 4, pp. 387–391, 2010, doi: 10.1016/j.aej.2010.07.004.
[9] D. Sibit and G. Handayani, "The Crosshole Sonic Logging (CSL) Measurement System to Measure the Quality of Physical Model of Bored Pile," *J. Phys. Conf. Ser.*, vol. 739, no. 1, 2016, doi: 10.1088/1742-6596/739/1/012051.
[10] X. Yu, M. Y. Abu-Farsakh, S. Yoon, C. Tsai, and Z. Zhang, "Implementation of LRFD of Drilled Shafts in Louisiana," *J. Infrastruct. Syst.*, vol. 18, no. 2, pp. 103–112, 2012, doi: 10.1061/(ASCE)IS.1943-555X.0000084.
[11] H. G. Poulos, "Tall building foundations: design methods and applications," *Innov. Infrastruct. Solut.*, vol. 1, no. 1, pp. 1–51, 2016, doi: 10.1007/s41062-016-0010-2.
[12] ASTM-D1143, "Standard Test Method for Piles Under Static Axial Compressive Load," *Am. Soc. Test. Mater.*, vol. 4, no. 8, pp. 1–12, 2010.
[13] D. A. Brown, J. P. Turner, and R. J. Castelli, *Drilled Shafts: Construction Procedures and LRFD Design Methods*, no. FHWA NHI-10-016. New York, 2010.
[14] NCHRP, "Load and Resistance Factor Design (LRFD) for Deep Foundations," Washington D.C., 2004.
[15] M. W. O'neill and L. C. Reese, *Drilled Shafts: Construction Procedures and Design Methods*. FHWA-IF-99-025, 1999.

[16] L. Stark T. J., Assem, P, "Improvement for Determining the Axial Capacity of Drilled Shafts in Shale in Illinois," Illinois, 2013.
[17] M. W. O'neill, F. C. Townsand, K. M. Hassan, A. Buller, and P. S. Chan, *Load Transfer for Drilled Shafts in Intermediate Geomaterials*. 1996.
[18] A. Alshenawy, W. Hamid, and A. Alnuaim, "Skin friction behavior of pile fully embedded in limestone," *Arab. J. Geosci.*, vol. 11, no. 2, pp. 1–7, 2018, doi: 10.1007/s12517-018-3386-9.
[19] S. K. Martin and K. Syngros, "Bored Pile Construction Challenges in Highly Variable Limestone for a Supertall Building," in *International Conference on Deep Foundations, Seepage Control and Remediation (41st Annual)*, 2016.
[20] T. Y. Chin and C. C. Meng, "Foundation Design and Construction in Limestone Formation: A Malaysian Consultant's Experience," in *International Symposium on Advances in Foundation Engineering (ISAFE 2013)*, 2013.
[21] E. L. Juvencio, F. R. Lopes, and A. L. L. S. Nunes, "An evaluation of the shaft resistance of piles embedded in gneissic rock," *Soils and Rocks*, vol. 40, no. 1, pp. 61–74, 2017.
[22] A. Alshenawy, W. Hamid, and A. Alnuaim, "Skin friction behavior of pile fully embedded in limestone," *Arab. J. Geosci.*, vol. 11, no. 2, pp. 1–7, 2018, doi: 10.1007/s12517-018-3386-9.
[23] S. Rezazadeh and A. Eslami, "Empirical methods for determining shaft bearing capacity of semi-deep foundations socketed in rocks," *J. Rock Mech. Geotech. Eng.*, vol. 9, no. 6, pp. 1140–1151, 2017, doi: 10.1016/j.jrmge.2017.06.003.
[24] L. Zhang, *Drilled Shafts in Rock: Analysis and Design*. Leiden: A.A.Balkema Publishers, 2004.
[25] L. Zhang, "Determination and applications of rock quality designation (RQD)," *J. Rock Mech. Geotech. Eng.*, vol. 8, no. 3, pp. 389–397, 2016, doi: 10.1016/j.jrmge.2015.11.008.
[26] SNI8460, "Standar Nasional Perancangan Geoteknik," *Badan Stand. Nas. Indones.*, pp. 1–323, 2017.